

of Zn^{65} and Zn^{67} are small suggests that a single-particle shell model with CM is appropriate in these cases, as discussed earlier. However, Kisslinger²⁴ has pointed out that odd zinc nuclei almost certainly cannot be described in terms of a pure configuration. In the lowest approximation the states are pure one-quasiparticle states, but this, however, is a poor approximation (see Ref. 2, Table VIII in Appendix). Thus the states must be described as quasiparticle-phonon admixtures. Although the values of Q_{65} and Q_{67} obtained by Kisslinger and Sorensen are not in accord with the measured values, Kisslinger and Kumar²⁵ have considered some new admixtures of phonons with quasiparticles which may change the values obtained within the framework of the model. In view of the large quadrupole moment of Zn^{63} , it is clear that a shell model with configuration mixing is not adequate and that some nuclear model which takes into account the collective effects in a consistent manner must be used.

²⁴ L. S. Kisslinger (private communication).

²⁵ L. S. Kisslinger and K. Kumar, *Phys. Rev. Letters* **19**, 1239 (1967).

At this point it is interesting to note that an old rule of thumb, namely, that the quadrupole moments of odd-neutron nuclei are approximately equal in magnitude to those of odd-proton nuclei with the same configuration, works well in the case of Zn^{63} . The closest nuclei with a $(1p_{3/2})^3$ proton configuration are As^{75} with $Q = +0.29$ b, Br^{79} with $Q = +0.31$ b and Br^{81} with $Q = +0.26$ b.

ACKNOWLEDGMENTS

The authors would like to acknowledge the important contributions made by many others to this research. Members of the University of Washington Nuclear Physics Laboratory cyclotron crew cooperated in the Zn^{63} production. P. W. Spence and R. L. Chaney provided assistance during the critical isotope transfer operation. Professor Howard Shugart of the University of California, Berkeley, kindly provided the computer program used in reducing the data. Jacob Jonson, Physics Department glassblower, displayed great skill and patience in making the numerous quartz pieces indispensable to this research.

Spin and Nuclear Moments of 55-min Cd^{105} and 49-min Cd^{111m} †

N. S. LAULAINEN* AND M. N. McDERMOTT

University of Washington, Seattle, Washington 98105

(Received 23 September 1968)

The hyperfine structures of the 3P_1 state of 55-min Cd^{105} and 49-min Cd^{111m} have been determined by the optical double-resonance technique. For Cd^{105} , the measurements yield a nuclear spin $I = \frac{5}{2}$, a dipole interaction constant $A_{105}(^3P_1) = -1025.9(2)$ MHz, and a quadrupole interaction constant $B_{105}(^3P_1) = -103.9(3)$ MHz. For Cd^{111m} , $I = \frac{5}{2}$, $A_{111m}(^3P_1) = -697.1(2)$ MHz, and $B_{111m}(^3P_1) = +202.3(5)$ MHz. If the hfs anomaly and quadrupole shielding effects are neglected, the nuclear magnetic dipole moments with diamagnetic correction are $\mu_{105} = -0.7385(2)\mu_N$ and $\mu_{111m} = -1.1040(4)\mu_N$, and the nuclear quadrupole moments are $Q_{105} = +0.43(4)$ b and $Q_{111m} = -0.85(9)$ b.

I. INTRODUCTION

IN the preceding paper¹ we discussed the extension of the optical double resonance technique to nuclei with half-lives $\gtrsim 1$ h and reported on an application of this technique to a measurement of the spin and nuclear moments of the 38-min Zn^{63} ground state. In this paper we report on a further application, the measurement of the spin and nuclear moments of the 55-min Cd^{105} ground state and the 49-min Cd^{111} isomeric state. The completion of this research brings to six the number of quadrupole moments which have been measured for

cadmium isotopes by the optical double-resonance technique. With these new measurements we are able to make a further test of Byron's² semiempirical expression for the quadrupole moments of odd-neutron nuclei.

II. EXPERIMENTAL TECHNIQUES

A. Double-Resonance Apparatus

The double resonance apparatus used in this work (Fig. 1) is nearly identical to that used in the Zn^{63} experiment. Unpolarized resonance radiation from an electrodeless cadmium discharge lamp is directed onto a heated cylindrical quartz absorption cell. The cadmium sample in the absorption cell is placed in a magnetic

† Work supported in part by the National Science Foundation.

* Present address: Erstes Physikalisches Institut der Universität Heidelberg, 69 Heidelberg, Germany.

¹ N. S. Laulainen and M. N. McDermott, preceding paper, *Phys. Rev.* **177**, 1606 (1968).

² F. W. Byron, Jr., M. N. McDermott, R. Novick, B. W. Perry, and E. B. Saloman, *Phys. Rev.* **136**, B1654 (1964).

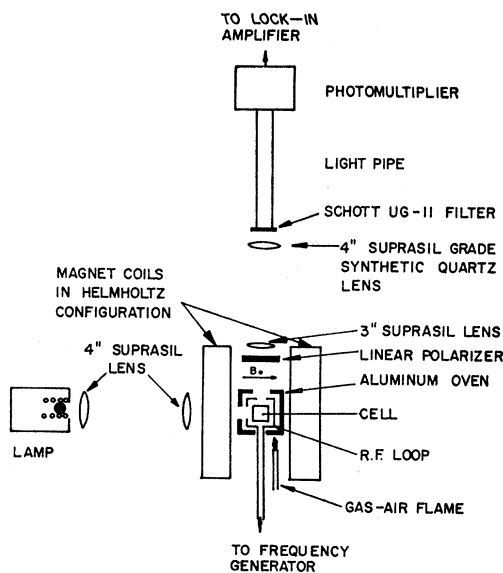


Fig. 1. Schematic diagram of the double-resonance apparatus.

field directed parallel to the incoming light. Light which is scattered at right angles to the field is analyzed by a linear polarizer which passes light polarized parallel to the field. A system of lenses focuses this light onto a photomultiplier through a uv-transmitting filter. With this arrangement any transition which results in a change in the intensity of scattered π light can be detected.

B. Sensitivity

The detection sensitivity of this apparatus for cadmium is considerably greater than that for zinc. The major reason for this is the greater oscillator strength of the cadmium resonance line. The observed light scatter from the apparatus can be used to place a lower limit on the number of atoms which can be detected. The shot noise in the photocurrent from the instrumental scatter competes with the signal from the light scattered by the atoms. With the level of instrumental scatter observed in this experiment the minimum detectable number of atoms is estimated to be 1×10^8 for Cd^{105} ($I = \frac{5}{2}$) and 5×10^8 for Cd^{111m} ($I = \frac{11}{2}$). In practice the minimum numbers observed were $\sim 1 \times 10^{10}$ for Cd^{105} and $\sim 5 \times 10^{10}$ for Cd^{111m} . The difference can be explained by the effects of light scatter from the stable cadmium isotopes and the Cd^{107} and Cd^{109} atoms present as contaminants. As shown in the next section the Cd^{107} and Cd^{109} atoms were each at least a factor of 16 more abundant than the Cd^{105} atoms immediately after production. The increased shot noise resulting from the light scatter from these other isotopes raises the estimated minimum detectable number of Cd^{105} atoms to $\sim 2 \times 10^9$ and that of Cd^{111m} to $\sim 1 \times 10^{10}$. The additional factor of 5 is within a combination of the uncertainties in the measured activities, the isotope recovery efficiency, and

the number of atoms actually in the vapor phase in the cell.

In the hfs measurements, cylindrical cells 2.8 cm in diam and 2.8 cm in length were used. This size closely approximates the volume defined by the illumination and detection lens systems. For such a cell 2×10^{14} cadmium atoms (roughly the total available sample per experiment) are in the vapor phase in equilibrium with an excess of the solid at 210°C . However, samples this small constitute less than a monolayer on the cell walls and at this temperature it is probable that many of the atoms adhere to the walls. In order to produce the maximum signal it was necessary to increase the temperature of the cell to about 350°C . The hfs measurements in Cd^{105} and Cd^{111m} were made with cells at this temperature.

The light sources were similar to those which have been used for cadmium previously.³ A lamp consisted of a quartz sphere 3 cm in diam which contained a small quantity of cadmium metal and a neon carrier gas at a pressure of about 1 Torr. It was excited by placing it directly in the tank coil of a Hartley oscillator run at 20 MHz. Under the best operating conditions the intensity in the 3261 \AA cadmium intercombination line was about 1.5 W.

C. Isotope Production and Cell Preparation

The Cd^{105} and Cd^{111m} were produced by the reactions $\text{Pd}^{104}(\alpha, 3n)\text{Cd}^{105}$ and $\text{Pd}^{110}(\alpha, 3n)\text{Cd}^{111m}$. A palladium foil was bombarded with 42-MeV α particles for about 75 min (or roughly one mean life of the Cd^{105} and Cd^{111m} isotopes) at a beam intensity of about $30 \mu\text{A}$. Counting measurements indicated that about 45 mCi of Cd^{105} (8×10^{12} atoms) and 180 mCi (3×10^{13} atoms) were produced compared with the 180 mCi yield of each isotope calculated from a mean reaction cross section of 1.5 b. This cross section was estimated from the expression⁴ $\bar{\sigma} = \pi R^2(1 - Zze^2/RE_\alpha)$, where $R = 1.4A^{1/3} + 2.2 \text{ f}$, Ze is the charge on the target nucleus, ze is the charge on the projectile, and E_α is the energy of the incident α .

The palladium foil was specified to have a cadmium contamination of less than 0.1 ppm. This was reduced by a factor of at least 4 as a result of a bakeout procedure. The foil was heated to 1050°C under vacuum for 5–6 days, then quickly sealed off in a quartz tube before it cooled. With the size foils used no more than 3×10^{14} stable cadmium atoms should have been present in the foil at the end of the bakeout.

An additional complication arose, however, from the fact that Cd^{107} and Cd^{109} were also produced in the palladium foil by the reactions $\text{Pd}^{106}(\alpha, 3n)\text{Cd}^{107}$ and $\text{Pd}^{108}(\alpha, 3n)\text{Cd}^{109}$. If it is assumed that the mean cross sections for producing Cd^{105} , Cd^{107} , Cd^{109} , and Cd^{111m} are the same, then, for a 75-min bombardment time, the numbers of the various cadmium isotopes produced

³ M. N. McDermott and R. Novick, Phys. Rev. **131**, 707 (1963).

⁴ R. H. Venter and W. E. Frahn, Ann. Phys. (N.Y.) **27**, 401 (1966).

bear the following relationship: $N(Cd^{107}) \simeq N(Cd^{109}) \simeq 4N(Cd^{105}) \simeq 4N(Cd^{111m})$. The factor of 4 difference between the number of Cd^{107} and Cd^{109} atoms and the number of Cd^{105} and Cd^{111m} atoms comes from two different sources. A factor of 1.5 arises because Cd^{107} and Cd^{109} do not decay appreciably during 75 min, whereas Cd^{105} and Cd^{111m} do. A further enhancement of Cd^{107} and Cd^{109} by a factor of 2.5 arises from the relative abundances of the target nuclei, namely, $Pd^{104}:Pd^{106}:Pd^{108}:Pd^{110} = 1:2.5:2.5:1$.

As actually observed, the resonance signals are consistent with $(\alpha, 3n)$ cross sections of $\bar{\sigma}(Cd^{107}) \simeq \bar{\sigma}(Cd^{109}) \simeq \bar{\sigma}(Cd^{111m}) \simeq 4\bar{\sigma}(Cd^{105})$. For a 75-min irradiation time and these relative cross sections $N(Cd^{107}) \simeq N(Cd^{109}) \simeq 4N(Cd^{111m}) \simeq 16N(Cd^{105})$ in accord with our observations.

The quartz vacuum system which was used in the transfer of the activity to the sample cell (Fig. 2) is a modified version of the one used in the Zn⁶³ experiment. Great care was taken to avoid stable cadmium contamination and to produce gas-free cells. Prior to a run the entire glass system was baked under vacuum for at least 24 h at 450°C. The quartzware including the scattering cell was further baked for 12 h at 1000°C. Neon was admitted and the scattering cell purged with a vigorous rf discharge in neon. The quartzware was then given a final bakeout at 1000°C for 12 h.

After irradiation the palladium foils were placed in a carbon crucible supported in a quartz T section by a tungsten wire, the system was sealed and evacuated, and the palladium was heated to melting by means of an induction heater. The cadmium activity was observed to distill from the palladium in less than 5 min and to collect on the walls of the quartz T section. Heating tapes and a hand torch were used to further distill the activity into a cooled U section filled with crushed quartz granules. A hand torch was used to transfer the activity from the U section to the cell. As a final step a

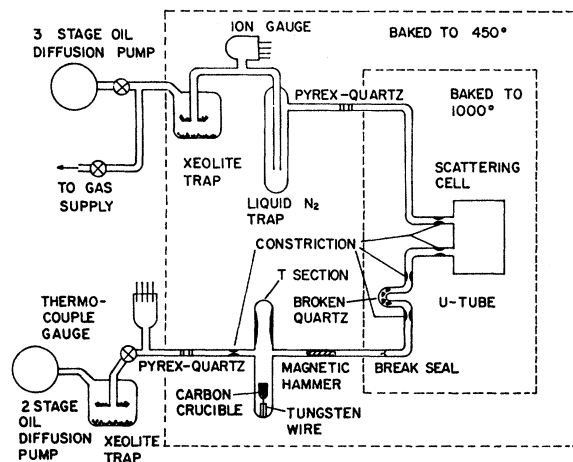


FIG. 2. Schematic diagram of the vacuum apparatus used in preparing the Cd^{105} and Cd^{111m} scattering cells.

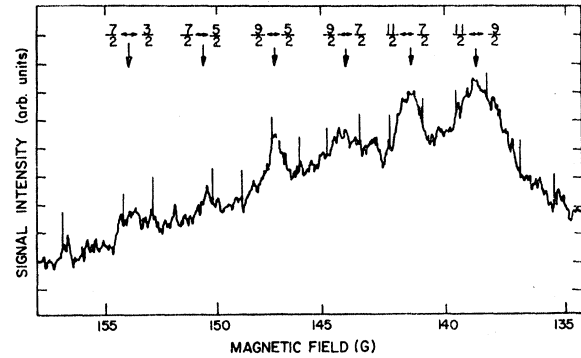


FIG. 3. Zeeman spectrum of the $F=11/2$ hyperfine level in Cd^{111m} at $\nu=10$ MHz. The transitions are labeled by the magnetic quantum numbers $m_F \leftrightarrow m_F'$ of the sublevels involved.

high-frequency discharge was produced in the cell by a Tesla coil. On the average about 1 h elapsed from the end of bombardment to the completion of the cell.

A survey of the activity in a cell and in other pieces of the isotope recovery apparatus indicated that about 50% of the cadmium activity was transferred into each cell. In view of the amount produced in the target it can be deduced that at the time a cell was completed it contained $\sim 6 \times 10^{12}$ Cd^{111m} atoms and $\sim 1.5 \times 10^{12}$ Cd^{105} atoms. The amount of stable cadmium in a cell was quite small and was generally less than the amount of Cd^{109} produced. As pointed out earlier substantial quantities of both Cd^{107} and Cd^{109} were present. $N(Cd^{107}) \simeq N(Cd^{109}) \simeq 8N(Cd^{111m}) \simeq 32N(Cd^{105})$ at the time a cell was completed, a condition which greatly complicated the spin search for Cd^{105} .

III. MEASUREMENTS

A. Nuclear Spin

Cd^{111m}

The spin determination for Cd^{111m} can be made on the basis of a set of Zeeman resonances (Fig. 3) observed at a frequency of 10 MHz and at fields of the order of 140 G. The resonance spectrum is well fit by assuming it results from transitions within a level with $F = \frac{1}{2}$. In general, in a state for which $J = 1$, $2F - 1$ resonances will be observed approximately symmetrically spaced about a central field of $B_0 = h\nu / (g_F \mu_0)$. ν is the rf frequency, g_F the Lande g factor for the hyperfine level, and μ_0 the Bohr magneton. The approximation involved is the neglect of terms of order higher than B_0^2 . The splittings between the three resonances which result from single-quantum transitions can be used to infer a value of B_0 which agrees closely with that expected for a level for which $g_F/g_J = 4/143$. Since $g_F/g_J = 1/[I(I+1)]$ for a state with $F = I$, a value of $I = \frac{1}{2}$ is established. No other spin possibilities lead to resonances which are close to the ones observed.

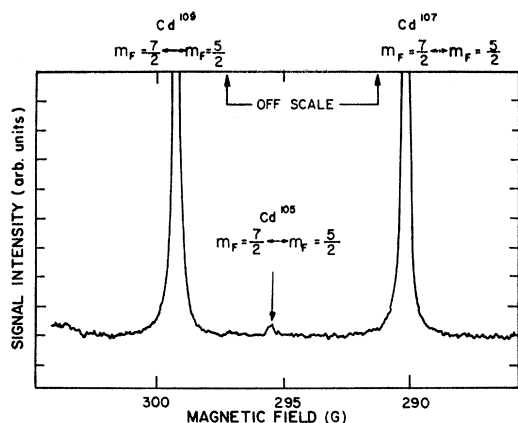


FIG. 4. Comparison of the $(7/2, 7/2) \leftrightarrow (7/2, 5/2)$ resonance in Cd^{107} and Cd^{109} to that of Cd^{105} at $\nu = 200$ MHz.

Although a complete resonance pattern should contain ten resonances corresponding to single-quantum transitions only three were obtained on the low-field side of B_0 . This was due partially to the fact that the individual Zeeman resonance strengths in a state for which $J=1$, $F=1\frac{1}{2}$, $I=1\frac{1}{2}$ are in the ratio 100:64:36:16:4. The resonances increase in strength in moving away from the central field B_0 . From the amplitude of the strong resonances it is immediately apparent that the resonances close to B_0 were too weak to be observed. No attempt was made to obtain the high-field portion of the pattern.

The chart recorder tracing of the resonance spectrum in Fig. 3 also shows resonance signals associated with two-quantum transitions. Under the experimental conditions which prevailed two-quantum transitions have resonance widths which are about one-half those of single-quantum transitions and are thus easily identified.

Additional evidence supporting the correctness of the nuclear spin assignment is provided by the fact that the positions of every resonance observed for a wide range of fields can be fit to better than 1 part in 10^4 by making use of the two hyperfine parameters A and B . This is true only under the assumption that the nuclear spin is $I=1\frac{1}{2}$. The spin determination is in accord with an earlier assignment based on the internal conversion coefficients and γ - γ correlation measurements.⁵

Cd^{105}

The spin determination for Cd^{105} was made considerably more difficult by the presence of Cd^{107} and Cd^{109} isotopes in the cell. Cd^{107} and Cd^{109} both have nuclear spin $I=5/2$. As pointed out earlier there were about 32 times more Cd^{107} and Cd^{109} atoms than Cd^{105} atoms at the time the cell was completed. This meant that if $I=5/2$ for

Cd^{105} and the magnetic moment of Cd^{105} was not substantially different from that for Cd^{107} and Cd^{109} , resonances in Cd^{105} would not be resolved from much stronger resonances in Cd^{107} and Cd^{109} at low magnetic fields. Even with this competition from the Cd^{107} and Cd^{109} resonances at low field, we were able to eliminate the possibilities $I=3/2$ and $I=7/2$ completely and to eliminate $I=5/2$ as a possibility for a nuclear dipole moment in the range $0.30\mu_N < |\mu_I| < 0.60\mu_N$.

Successful identification of the nuclear spin of Cd^{105} was possible only at higher fields where the Cd^{107} and Cd^{109} resonances were quite well resolved. Four resonances were observed at fields of 295.5, 307.8, 270.2 and 388.9 G and a frequency of 200 MHz, and one resonance was observed at 281.5 G and a frequency of 120 MHz. In each case the resonance identified as belonging to Cd^{105} was bracketed by two resonances, one in Cd^{107} and one in Cd^{109} . The two bracketing resonances always resulted from transitions $(F, m_F) \leftrightarrow (F, m_F')$ in which F , m_F and m_F' were the same for both isotopes. Taken in sequence the five resonances listed occurred between the Cd^{107} and Cd^{109} resonances for the $(\frac{7}{2}, \frac{7}{2}) \leftrightarrow (\frac{7}{2}, \frac{5}{2})$, $(\frac{7}{2}, \frac{5}{2}) \leftrightarrow (\frac{7}{2}, \frac{3}{2})$, $(\frac{7}{2}, -\frac{3}{2}) \leftrightarrow (\frac{7}{2}, -\frac{5}{2})$, $(\frac{7}{2}, -\frac{5}{2}) \leftrightarrow (\frac{7}{2}, -\frac{7}{2})$ and $(\frac{5}{2}, \frac{5}{2}) \leftrightarrow (\frac{5}{2}, \frac{3}{2})$ transitions. Figure 4 shows a chart recorder tracing which offers a comparison of the resonance strengths in Cd^{107} and Cd^{109} to that in Cd^{105} for the $(\frac{7}{2}, \frac{7}{2}) \leftrightarrow (\frac{7}{2}, \frac{5}{2})$ transition. The separation between the Cd^{105} resonances at 200 MHz is precisely that expected for transitions in a state with $F=7/2$, $I=5/2$, and $g_F/g_J=9/7$. If the resonance located at $\nu=120$ MHz and $B=281.5$ G is followed to low fields, it is found to move under the $(\frac{5}{2}, \frac{5}{2}) \leftrightarrow (\frac{5}{2}, \frac{3}{2})$ resonance of Cd^{109} . This observation serves to identify the Cd^{105} resonance as one belonging to the $F=5/2$, $I=5/2$ hyperfine level. Additional

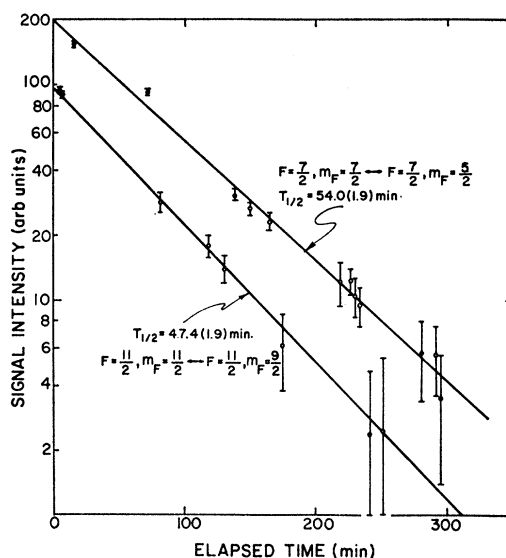


FIG. 5. Resonance amplitudes as a function of time for the $(11/2, 11/2) \leftrightarrow (11/2, 9/2)$ resonance in Cd^{113m} and the $(7/2, 7/2) \leftrightarrow (7/2, 5/2)$ resonance in Cd^{105} .

⁵ Nuclear Data Sheets, compiled by K. Way *et al.* (Printing and Publishing Office, National Academy of Sciences—National Research Council, Washington, D.C. 20025, 1960).

TABLE I. Resonance fields and frequencies used in the determination of the $\text{Cd}^{111m}(5s5p)^3P_1$ hfs interaction constants A and B .

Transition	Number of resonance pairs	Magnetic field (G)	Frequency (MHz)
$(11/2, 11/2) \leftrightarrow (11/2, 9/2)$	1	138.575(80)	10.0000(5)
$(11/2, 9/2) \leftrightarrow (11/2, 7/2)$	1	144.117(150)	10.0000(5)
$(11/2, 11/2) \leftrightarrow (11/2, 9/2)$	4	271.661(15)	24.0000(5)
$(13/2, 13/2) \leftrightarrow (13/2, 11/2)$	1	323.681(3)	120.0000(5)
$(11/2, 11/2) \leftrightarrow (11/2, 9/2)$	1	350.432(12)	35.0000(5)
$(13/2, 13/2) \leftrightarrow (13/2, 11/2)$	1	323.658(40)	120.0000(5)
$(11/2, 11/2) \leftrightarrow (11/2, 9/2)$	1	271.647(15)	24.0000(5)
$(11/2, 9/2) \leftrightarrow (11/2, 7/2)$	1	293.997(50)	24.0000(5)

evidence supporting this assignment was the observation of this same resonance located between the $(\frac{5}{2}, \frac{5}{2}) \leftrightarrow (\frac{5}{2}, \frac{3}{2})$ resonances of Cd^{107} and Cd^{109} at $\nu=200$ HMz. From the number of individual resonances observed and the field dependence of the Cd^{105} Zeeman spectrum, the nuclear spin of Cd^{105} is unambiguously determined to be $I=\frac{5}{2}$.

Unmistakable identification of the $I=\frac{1}{2}$ signal with Cd^{111m} and the $I=\frac{5}{2}$ signals with Cd^{105} was made by carefully observing the decay of the amplitude of the Zeeman transitions $(\frac{1}{2}, \frac{1}{2}) \leftrightarrow (\frac{1}{2}, \frac{3}{2})$ in Cd^{111m} and $(\frac{7}{2}, \frac{7}{2}) \leftrightarrow (\frac{7}{2}, \frac{5}{2})$ in Cd^{105} . The resonance amplitudes as a function of time are shown in Fig. 5 fitted to exponential decay curves. The least-squares fits correspond to half-lives of 47.4(1.9) min and 54.0(1.9) min in good agreement with the accepted values of 48.6(3) min⁶ for Cd^{111m} and 54.7(8) min⁷ for Cd^{105} .

C. Hyperfine Structure

The final determinations of the Cd^{111m} and Cd^{105} hfs constants are based on measurements of the transitions summarized in Tables I and II. For Cd^{111m} the frequencies at resonance were 10, 24, 35, and 120 MHz and the magnetic fields ranged from 138 to 351 G. Chart recorder tracings of the strongest Zeeman transitions in the $F=\frac{3}{2}$ and $F=\frac{1}{2}$ levels of Cd^{111m} are shown in Fig. 6. Figure 7 shows the chart recorder tracings of the strongest Zeeman transitions in the $F=\frac{7}{2}$ and $F=\frac{5}{2}$ levels of Cd^{105} . In each case the final determination of the hfs constants is based on a set of resonance field and frequency measurements which exclude signals with signal-to-noise ratios of less than 5. The signal-to-noise ratios for the resonances included ranged from about 5 to 15 and the resonance widths were typically ~ 200

TABLE II. Resonance fields and frequencies used in the determination of the $\text{Cd}^{105}(5s5p)^3P_1$ hfs interaction constants A and B .

Transition	Number of resonance pairs	Magnetic field (G)	Frequency (MHz)
$(7/2, 7/2) \leftrightarrow (7/2, 5/2)$	5	295.504(2)	200.0000(5)
$(7/2, 7/2) \leftrightarrow (7/2, 5/2)$	1	295.506(7)	200.0000(5)
$(5/2, 5/2) \leftrightarrow (5/2, 3/2)$	1	281.497(20)	120.0000(5)
$(7/2, -5/2) \leftrightarrow (5/2, -7/2)$	1	388.908(50)	200.0000(5)
$(7/2, 7/2) \leftrightarrow (7/2, 5/2)$	1	295.505(7)	200.0000(5)
$(7/2, 5/2) \leftrightarrow (7/2, 3/2)$	1	307.806(12)	200.0000(5)
$(7/2, -3/2) \leftrightarrow (7/2, -5/2)$	1	370.169(30)	200.0000(5)
$(7/2, -5/2) \leftrightarrow (7/2, -7/2)$	1	388.884(30)	200.0000(5)
$(5/2, 5/2) \leftrightarrow (5/2, 3/2)$	1	386.763(10)	200.0000(5)

⁶ A. C. Helmholtz, R. W. Hayward, and C. L. McGinnis, Phys. Rev. **75**, 1469 (A) (1949).

⁷ F. A. Johnson, Can. J. Phys. **31**, 1137 (1953).

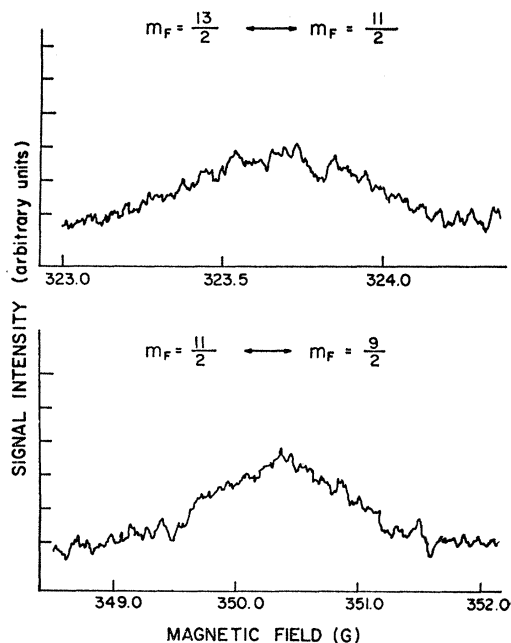


FIG. 6. Intermediate-field Zeeman transitions in the $F=13/2$ (top) and $F=11/2$ (bottom) hyperfine levels of $\text{Cd}^{111\text{m}}$ at $\nu=200$ MHz and $\nu=35$ MHz, respectively.

kHz for $\text{Cd}^{111\text{m}}$ and ~ 220 kHz for Cd^{106} . The rf power levels were sufficiently high to account for the observed widths.

Calibration of the magnetic field was carried out by measuring the frequency of the Zeeman resonance in the 3P_1 state of the spin $I=0$ cadmium isotope contaminants as a function of magnet current. This was done im-

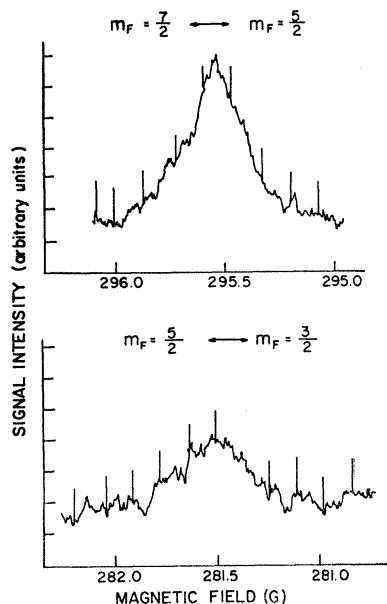


FIG. 7. Intermediate-field Zeeman transitions in the $F=7/2$ (top) and $F=5/2$ (bottom) hyperfine levels of Cd^{106} at $\nu=200$ MHz and $\nu=120$ MHz, respectively.

TABLE III. Constants used in evaluating the second-order hfs corrections.

Constant	Value of the constant for cadmium
a_1	0.5401(8)
a_2	0.8416(6)
ξ	1.034(10)
η	1.094(10)
$5\theta(1-\delta)(1-\epsilon)$	6.42(8)

mediately after the sample had decayed below a useful level. The position of the cell was not changed and the range of currents was the same as that employed in the experiment. In the determination of the hfs constants the magnetic field need not be known other than in units of the spin $I=0$ isotope frequency except for the small term $g_I\mu_0 B_0/h$. For this term we use $B_0 = h\nu/(g_I\mu_0)$ and the value $g_I = 1.599847(9)$.⁸

A two-parameter fit was made to the observed resonances. The parameters were the magnetic dipole interaction constant A and the quadrupole interaction constant B in the hyperfine Hamiltonian

$$\mathcal{H} = \frac{1}{2}khA + hB \frac{\frac{3}{4}k(k+1) - I(I+1)J(J+1)}{2I(2I-1)J(2J-1)} + g_I\mu_0\mathbf{J}\cdot\mathbf{B} + g_I\mu_0\mathbf{I}\cdot\mathbf{B}. \quad (1)$$

$k = F(F+1) - I(I+1) - J(J+1)$. The computation was carried out through the terms second order in perturbation theory which connect the states 3P_2 , 3P_1 , and 3P_0 of the fine-structure multiplet.⁹ This was accomplished by means of a modified¹⁰ version of the computer program HYPERFINE 4-94 originally developed by the Berkeley atomic-beam group. The constants used in evaluating the fine-structure corrections are given in Table III and are taken from a paper by Lurio.¹¹ The

TABLE IV. Individual electron hyperfine coupling constants for $\text{Cd}^{111\text{m}}$ and Cd^{106} .

Constant	Value of the constant in MHz	
	$\text{Cd}^{111\text{m}}$	Cd^{106}
a_s	-2093(4)	-3080(6)
$a_{1/2}$	-287(1)	-422(2)
$a_{3/2}$	-44(2)	-66(3)
$b_{3/2}$	-363(20)	+186(10)

⁸ P. Thaddeus and R. Novick, Phys. Rev. **126**, 1774 (1962).

⁹ A. Lurio, M. Mandel, and R. Novick, Phys. Rev. **126**, 1758 (1962).

¹⁰ N. S. Laulainen, Ph.D. thesis, University of Washington (unpublished).

¹¹ A. Lurio, Phys. Rev. **142**, 46 (1966).

individual electron hyperfine constants used are given in Table IV.

The values of the hfs coupling constants which gave the best fit to the data are listed in Table V. The "uncorrected" constants are those obtained before applying the fine-structure corrections. The "low-field" constants are those which would be determined from direct hyperfine transitions at zero-field and first-order perturbation theory. Only the corrections proportional to the first and second power of the applied field are retained in the calculation. The "isolated" constants include the corrections independent of the field as well. These are the constants which are found if *all* fine-structure corrections are made and are the constants from which the nuclear moments should be calculated. The errors quoted are four times the standard deviation for each constant as determined by the goodness of the fit. The uncertainty in the location of each resonance was taken to be $\Delta H = \Delta H_{\text{res}} / [2\sqrt{n(S/N)}]$, where ΔH_{res} is the width of the resonance, n is the number of resonance pairs used in determining the line centers and (S/N) is the signal-to-noise ratio of the resonance. The weight given each resonance is related to the value of ΔH assigned. It is important to note that the values of A and B are not changed significantly if all the data points are included and if all the resonances are weighted equally.

The sign of the dipole constant A was determined by a separate experiment which used circularly polarized incident radiation.³ For Cd^{111m} the resonance in the $F = \frac{1}{2}$ level which appeared at the lowest field was observed to disappear for σ^- light and was enhanced for σ^+ light. This observation is sufficient to establish that the hfs of Cd^{111m} is inverted and consequently that A_{111m} is negative. Similarly, for Cd^{105} the low-field resonance in the $F = \frac{1}{2}$ level was extinguished for σ^- light and enhanced for σ^+ light. Thus the hfs of Cd^{105} is inverted and hence A_{105} is negative.

IV. NUCLEAR MOMENTS

A. Measured Moments

The magnetic dipole moments of Cd^{111m} and Cd^{105} can be obtained from the known moment for Cd^{109} and the

TABLE V. Values of the hfs coupling constants of the $(5s5p)^3P_1$ state of Cd^{111m} and Cd^{105} .

	Uncorrected	Low field	Isolated
A_{111m} (MHz)	-697.2(2)	-697.1(2)	-697.1(2)
B_{111m} (MHz)	+204.5(5)	+201.2(5)	+202.3(5)
χ^2	8.5	5.4	5.4
A_{105} (MHz)	-1025.8(2)	-1025.9(2)	-1025.9(2)
B_{105} (MHz)	-103.5	-104.4(3)	-103.9(3)
χ^2	1.4	3.7	3.6

ratios of the dipole interaction constants of Cd^{111m} and Cd^{105} to that of Cd^{109} .¹² Using $A_{109} = -1148.748(7)$ MHz¹³ and $\mu_{109} = -0.82701(20)\mu_N$,^{14,15} we obtain the values of the dipole moments of Cd^{111m} and Cd^{105} :

$$\mu_{111m} = -1.1040(4)\mu_N,$$

and

$$\mu_{105} = -0.7385(2)\mu_N.$$

A diamagnetic correction of 0.48% is included. In these derivations the possible existence of hfs anomalies has been neglected.

The ratio of the quadrupole moments of two isotopes of the same element is equal to the ratio of their quadrupole coupling constants, independent of shielding corrections. With $B_{109} = -165.143(5)$ MHz¹³ we find

$$Q_{111m}/Q_{109} = -1.2250(30)$$

and

$$Q_{105}/Q_{109} = 0.6292(18).$$

The calculation of the absolute value of Q is based on the value of $\langle r^{-3} \rangle_{\text{ave}}$ for the $p_{3/2}$ electron. McDermott and Novick³ have estimated $\langle r^{-3} \rangle_{\text{ave}}$ from measurements in the 3P_2 and 3P_1 states of Cd^{111} and find $Q_{109} = 0.78(10)$ b. However, in their estimates of $\langle r^{-3} \rangle_{\text{ave}}$ from the fine structure they have ignored the fact that the radial wave functions of the p electron in the triplet and singlet states may be different. Therefore we have recalculated the value of Q_{109} using Lurio's¹¹ extension of the Breit-Wills¹⁶ theory of the hfs of the sl configuration. This modification of the Breit-Wills theory introduces a parameter λ (the ratio of the off-diagonal to the diagonal matrix elements of the spin-orbit operator) which for cadmium is $\lambda = 0.7618$. Lurio¹¹ has estimated the dipole interaction constant $a_{3/2}$ for the $p_{3/2}$ electron from the 3P_2 and 3P_1 hfs of Cd^{111} and finds $a_{3/2}(111) = a_{3/2}^{TT} = 266.6$ MHz. a^{TT} refers to the diagonal matrix element of the dipole interaction for the triplet state.

An inspection of Kopfermann's¹² expression for $a_{3/2}$ shows that we can deduce $a_{3/2}$ for Cd^{109} from $a_{3/2}(109) = [g_I(109)/g_I(111)]a_{3/2}(111)$. With the value^{14,15} of $g_I(109)/g_I(111) = 0.278321$ we obtain $a_{3/2}(109) = a_{3/2}^{TT} = 74.2$ MHz. We can also obtain $a_{3/2}$ from the fine structure.¹² The Wolfe¹⁷ corrected spin-orbit parameter is $\zeta_p = 1004$ cm⁻¹. With $HZ_i/F_{3/2} = 48.4$ from Schwartz¹⁸ and $g_I = 1.802 \times 10^{-4}$, we obtain $a_{3/2}(109) = a_{3/2}^{ST} = 59.8$ MHz from the fine structure. $a_{3/2}^{ST}$ refers to the off-diagonal matrix element of the dipole interaction between singlet and triplet states. From $B_{109} = -165.143(5)$ MHz we obtain $b_{3/2} = 294.7$ MHz. If we combine the expres-

¹² H. Kopfermann, *Nuclear Moments* (Academic Press Inc., New York, 1958), 2nd ed.

¹³ P. Thaddeus and M. N. McDermott, *Phys. Rev.* **132**, 1186 (1963).

¹⁴ M. Leduc and J. Brossel, *Compt. Rend.* **266**, 12 (1968).

¹⁵ P. W. Spence, Ph.D. thesis, University of Washington, 1968, (unpublished).

¹⁶ G. Breit and L. A. Wills, *Phys. Rev.* **44**, 470 (1933).

¹⁷ H. C. Wolfe, *Phys. Rev.* **41**, 443 (1932).

¹⁸ C. Schwartz, *Phys. Rev.* **97**, 380 (1955); **105**, 173 (1957).

TABLE VI. Magnetic dipole moment predictions for Cd¹⁰⁵ and Cd^{111m} based on the shell model with configuration mixing. C is a parameter proportional to the strength of the pairing interaction.

Isotope	Spin	Protons	Configuration Neutrons	Single particle	Magnetic moment		Experiment
					C=20 MeV	C=30 MeV	
Cd ¹⁰⁵	5/2	(2p _{1/2}) ² (1g _{9/2}) ⁸	(2d _{5/2}) ⁵ (1g _{7/2}) ² (1h _{11/2}) ⁰		-0.80μ _N	-0.52μ _N	
			(2d _{5/2}) ⁵ (1g _{7/2}) ⁰ (1h _{11/2}) ²		-0.65	-0.32	
			(2d _{5/2}) ³ (1g _{7/2}) ² (1h _{11/2}) ²	-1.913μ _N	-1.11	-0.90	-0.7385(2)μ _N
			(2d _{5/2}) ³ (1g _{7/2}) ⁰ (1h _{11/2}) ⁴		-0.95	-0.69	
Cd ^{111m}	11/2	(2p _{1/2}) ² (1g _{9/2}) ⁸	(2d _{5/2}) ⁶ (1g _{7/2}) ⁶ (1h _{11/2}) ¹		-1.34	-1.20	
			(2d _{5/2}) ⁶ (1g _{7/2}) ⁴ (1h _{11/2}) ³	-1.913μ _N	-1.08	-0.86	-1.1040(4)μ _N
			(2d _{5/2}) ⁶ (1g _{7/2}) ² (1h _{11/2}) ⁵		-0.83	-0.54	

sions for $a_{3/2}$ and $b_{3/2}$ given by Kopfermann we find

$$Q = (8/3) (\mu_0/e)^2 g_I (F_{3/2}/R) (b_{3/2}/a_{3/2}),$$

where $F_{3/2}$ and R are relativistic correction factors. With $F_{3/2}/R=0.963$,¹⁸ we obtain $Q=0.69$ b from the hyperfine structure. In order to calculate Q from the fine structure, the value $a_{3/2}^{ST}$ must be corrected so that the same value of $\langle r^{-3} \rangle_{\text{ave}}$ is used for both $a_{3/2}$ and $b_{3/2}$, namely $\langle r^{-3} \rangle^{TT}$. The result is $a_{3/2}^{TT} = a_{3/2}^{ST}/\lambda = 78.5$ MHz; hence $Q=0.65$ b from the fine structure. The agreement between these two values is quite good—much better than if the difference between the p -electron radial wave functions in the triplet and singlet states is ignored. We choose as more likely to be correct the value of the quadrupole moment obtained from the hyperfine-structure estimate, $Q_{109}=0.69(7)$ b. The quoted uncertainty is large enough to include the fine-structure-based estimate. The Cd^{111m} and Cd¹⁰⁵ quadrupole moments are then

$$Q_{111m} = -0.85(9) \text{ b}$$

and

$$Q_{105} = 0.43(4) \text{ b}.$$

We can also reevaluate the quadrupole moments of Cd¹⁰⁷, Cd^{113m}, and Cd^{115m}. With $Q_{107}/Q_{109}=0.98871(4)$,¹³ $Q_{113m}/Q_{109}=-1.02371(4)$ ² and $Q_{115m}/Q_{109}=-0.79(3)$ ¹⁹ we find

$$Q_{107} = 0.68(7) \text{ b},$$

$$Q_{113m} = -0.71(7) \text{ b},$$

$$Q_{115m} = -0.55(6) \text{ b}.$$

The quoted error includes the range of values resulting

¹⁹ M. N. McDermott, R. Novick, B. W. Perry, and E. B. Saloman, Phys. Rev. **134**, B25 (1964).

²⁰ R. M. Sternheimer, Phys. Rev. **164**, 10 (1967).

from various estimates of $\langle r^{-3} \rangle_{\text{ave}}$. Sternheimer-type²⁰ shielding corrections have been neglected.

B. Theoretical Moments

The configuration mixing model of Noya, Arima, and Horie²¹ has been used to calculate the nuclear moments of Cd^{111m} and Cd¹⁰⁵. A harmonic-oscillator central potential is assumed and values of the nuclear pairing energy parameter $C=20$ and 30 MeV (the values which best fit the nuclear binding energy in the region of light and medium mass nuclei) are chosen. The results for the dipole moments of Cd¹⁰⁵ and Cd^{111m} are summarized in Table VI. The ground-state proton configuration for Cd¹⁰⁷ and Cd¹¹¹ which has been previously assumed² is $(2p_{1/2})^2(1g_{9/2})^8$. The assumed neutron configurations are $(2d_{5/2})^5(1g_{7/2})^4$ for Cd¹⁰⁷ and $(2d_{5/2})^6(1g_{7/2})^6(3s_{1/2})^1$ for Cd^{111m}. These configurations give the correct spins but a rather poor moment prediction for one or the other of the isotopes if the same value of C is used for both.

Recent studies^{22,23} of (d, p) and (d, t) reactions on Pd, Cd, and Sn isotopes suggest that the $h_{11/2}$ neutron level lies lower than has been usually assumed. In Cd¹¹⁴ the stripping results seem to show $h_{11/2}$ and $d_{5/2}$ levels which are about $\frac{2}{3}$ full and a $g_{7/2}$ level which is about $\frac{1}{2}$ full.

This discovery has been followed by a reevaluation¹⁵ of the predictions of the configuration mixing model for the magnetic moments of cadmium isotopes other than Cd¹⁰⁵ and Cd^{111m}. In the reevaluation not only the moments were considered but also the magnetic hyperfine-structure anomalies for Cd¹⁰⁷, Cd¹⁰⁹, Cd¹¹¹, and Cd¹¹³. The anomalies are generally more sensitive to the assumed configurations than are the moments. The

²¹ H. Noya, A. Arima, and H. Horie, Progr. Theoret. Phys. (Kyoto) Suppl. **8**, 33 (1958).

²² J. B. Moorhead, B. L. Cohen, and R. A. Moyer, Phys. Rev. **165**, 1287 (1968).

²³ L. H. Goldman and J. Kremenek, Bull. Am. Phys. Soc. **13**, 120 (1968).

conclusions of this study strongly tend to support the choice of configurations with a larger number of $h_{11/2}$ neutrons. In particular the choices $(2d_{5/2})^5(1h_{11/2})^4$ for Cd¹⁰⁷ and $(2d_{5/2})^6(1g_{7/2})^2(1h_{11/2})^4(1s_{1/2})^1$ for Cd¹¹¹ give the "best fit" to the moment and anomaly data for C in the range of 20–30 MeV.

With the foregoing results in mind we have calculated the magnetic moments for Cd¹⁰⁵ and Cd^{111m} for configurations which involve minimum change from those for Cd¹⁰⁷ and Cd¹¹¹. The values are presented in Table VI. As can be seen the configuration $(2d_{5/2})^5(1h_{11/2})^2$ for Cd¹⁰⁵ gives a calculated moment $\mu_{105}(\text{calc}) = -0.65\mu_N$ for $C=20$ MeV in fair agreement with the experimental value $\mu_{105} = -0.74\mu_N$. This configuration is preferred over those containing terms $(2d_{5/2})^3$ because of the measured large positive quadrupole moment. As illustrated by the case of Zn⁶⁵ a half-filled shell can lead to a nearly zero quadrupole moment even in cases which appear to have collective features.

For Cd^{111m} the configuration $(2d_{5/2})^6(1g_{7/2})^2(1h_{11/2})^5$ gives $\mu_{111m}(\text{calc}) = -0.83\mu_N$ for $C=20$ MeV in rather poor agreement with the measured value $\mu_{111m} = -1.10\mu_N$. The configuration $(2d_{5/2})^6(1g_{7/2})^4(1h_{11/2})^3$ is also acceptable and gives $\mu_{111m}(\text{calc}) = -1.08\mu_N$ for $C=20$ MeV in much better agreement. The existence of a large negative quadrupole moment for Cd^{111m} is a rather strong empirical argument against considering configurations which contain more than a half-filled $h_{11/2}$ shell. On the whole it is felt that the differences between the moments predicted for various configurations are not large enough nor is the configuration mixing model reliable enough to enable a choice of configuration to be made on the basis of the measured moments alone.

For the quadrupole moments of the cadmium isotopes the predictions of the CM model are quite unsatisfactory. McDermott and Novick⁶ have calculated the quadrupole moment of Cd¹⁰⁹ with the CM model with $C=30$ MeV and have found $Q_{109}(\text{calc}) = 0.10$ b. The experimental result is $Q_{109} = 0.69(7)$ b. The measured quadrupole moment is many times that expected for a

single particle and suggests collective effects are important. Despite this evident collective nature Byron² was able to reproduce the known quadrupole moments for the cadmium isotopes by means of a semiempirical formula based on the shell model,

$$Q = -[(2j+1-2N)/(2j+2)]\tilde{Q}_0.$$

j is the angular momentum of the last odd nucleon, N is the number of nucleons in the same shell-model state as the last odd nucleon, and \tilde{Q}_0 is a parameter to be determined empirically from isotopes for which the quadrupole moment is known. \tilde{Q}_0 is expected to be nearly constant for all isotopes and isomers of a given element.

In applying this formula to cadmium one possibility is to use a value of \tilde{Q}_0 which is the average value \tilde{Q}_0 for all previously measured cadmium isotopes and isomers. In addition to evaluating \tilde{Q}_0 it is further necessary to make a consistent choice of ground-state neutron configurations. If we adopt the ones given by Byron *et al.*² (Table VII) for Cd¹⁰⁷, Cd¹⁰⁹, Cd^{113m}, and Cd^{115m} we find a reasonably constant value for \tilde{Q}_0 and an average value of $\tilde{Q}_0 = 1.12$ b. If Q_{111m} is assumed to have a $(1h_{11/2})^1$ neutron configuration then $Q_{111m}(\text{calc}) = -(10/13)\tilde{Q}_0 = -0.85$ b. For a $(2d_{5/2})^5$ neutron configuration $\tilde{Q}_{0105}(\text{calc}) = (4/7)\tilde{Q}_0 = 0.63$ b. These results are in reasonable accord with the measured values of $Q_{111m} = -0.85(9)$ b and $Q_{105} = 0.43(4)$ b.

The formula is ambiguous and no longer useful if the configurations which give good agreement for the moments and anomalies are used. As seen in Table VII the isomeric states give values of \tilde{Q}_0 which differ wildly from the ground-state \tilde{Q}_0 values and do not even agree well among themselves. This result casts considerable doubt on the general utility of Eq. (2). The earlier success of Eq. (2) in predicting the cadmium quadrupole moments appears to have rested on a particularly fortunate choice of configurations which may not have been correct.

More detailed models such as the pairing plus quadrupole model of Kisslinger and Sorensen²⁴ have been used to calculate quadrupole moments for Cd¹⁰⁷ $Q_{107} = 0.75$ b, and for Cd¹⁰⁹ $Q_{109} = 0.79$ b which are in reasonably good agreement with experiment. These calculations have not yet been extended to Cd¹⁰⁵ or Cd^{111m}.

ACKNOWLEDGMENTS

We are pleased to acknowledge the valuable assistance of David Rump in taking the data for these experiments. Numerous members of the cyclotron crew of the University of Washington are to be thanked for the time which they contributed to the necessary isotope-production runs. We are also grateful for the support given this project by Jacob Jonson and Robert Morley of the Physics Department glass shop.

²⁴ L. S. Kisslinger and R. A. Sorensen, Rev. Mod. Phys. **35**, 833 (1963).

TABLE VII. The values of the parameter \tilde{Q}_0 as computed for the "old" neutron configurations used in earlier work and from the "new" configurations which give the best values for the magnetic moments and hyperfine-structure anomalies.

Isotope	Old configuration	\tilde{Q}_0 (b)	New configuration	\tilde{Q}_0 (b)
Cd ¹⁰⁵	$(2d_{5/2})^5$	0.75	$(2d_{5/2})^5$	0.75
Cd ¹⁰⁷	$(2d_{5/2})^5$	1.19	$(2d_{5/2})^5$	1.19
Cd ¹⁰⁹	$(2d_{5/2})^5$	1.20	$(2d_{5/2})^5$	1.20
Cd ^{111m}	$(1h_{11/2})^1$	1.10	$(1h_{11/2})^5$	5.5
Cd ^{113m}	$(1h_{11/2})^1$	0.92	$(1h_{11/2})^5$	4.6
Cd ^{115m}	$(1h_{11/2})^3$	1.19	$(1h_{11/2})^5$	3.6